Interference enhanced Raman spectroscopy of ultra thin crystalline Ge films

S. Kanakaraju[1], A. K. Sood[2] and S. Mohan[1,3]

[1]Department of Instrumentation, Indian Institute of Science, Bangalore 560 012, India
[2]Department of Physics, Indian Institute of Science, Bangalore 560 012, India
[3]C.S.I.O, Chandigarh, India

We report Raman study of ultra thin Ge films using interference enhanced Raman scattering which uses a trilayer structure of Al, CeO_2 and crystalline Ge films. The use of CeO_2 allows the growth of crystalline Ge films at relatively low substrate temperatures (300°C). With a decrease of Ge film thickness, the Raman line exhibits an increased red shift of the peak position and line broadening. The latter can be quantitatively explained on the basis of phonon confinement in the growth direction. Raman spectra of the 2 nm and 4 nm thick Ge films show shoulder at -280 cm^{-1} which could be attributed to surface phonons. The changes in the Raman shift as a function of thickness showed that the films were compressively strained up to a thickness of -7 nm beyond which the strain is released.

SEMICONDUCTING low-dimensional systems are attracting a lot of interest due to their novel behaviour arising from quantum size effects on electronic and vibrational states[1–11]. Properties of these structures are very sensitive to their microstructure, crystallinity, composition and nature of the interfaces. A variety of experimental techniques are being employed for their characterization. Among them, Raman scattering has proved to be a powerful probe in their characterization as well as to understand electron–phonon interactions[7,8]. Raman scattering can probe the structure, degree of crystallinity, composition, strain and quality of interfaces. Raman studies of semiconductor superlattices have revealed a number of interesting phenomena such as interface modes', confined optical phonons[10] and folded acoustic phonons". For example, our studies" had shown that in GaAs–AlAs superlattices, the confined longitudinal optical Raman phonons created via either deformation potential or Frohlich electron–phonon interaction are different. Resonance Raman scattering from these superlattices also revealed interface phonons which have frequencies close to the optical phonons of bulk GaAs and AlAs. *In situ* Raman monitoring of thin film growth has shown band bending during the formation of heterostructure[12], order–disorder transition during the film growth[13], and reaction in compound semiconductors[14–16]. In the simplest picture[17,18]; the phonon wave functions are confined in a nano crystal or thin films, while retaining the bulk dispersion relations. This confinement results in the breakdown of wavevector selection rules and hence the Raman line is asymmetrically broadened and is red-shifted (if the phonon frequency ω is a decreasing function of q) or blue shifted (if ω is an increasing function of q). In earlier theoretical description[19] of phonons of a nanocrystal using classical dielectric model, the phonon amplitude is coupled to the electrostatic potential via the Frolich interaction, but phonon dispersion is neglected. The use of spherical boundary condition results in confined longitudinal and surface eigenmodes. Recently, Roca *et al.*[20] included the dispersion of phonons in their theory of vibrational modes of a nanocrystal together with the appropriate mechanical as well as electromagnetic boundary conditions. Their prediction of coupling of the optical longitudinal and transverse modes was recently verified in Raman scattering of PbS nanocrystals with radii of 2 nm (ref. 21). Such confinement-induced changes in the Raman spectra as well as Raman characterization of growth and interfaces of ultra thin films have not been sufficiently investigated, This is because conventional non-resonant Raman backscattering of ultra thin films and their interfaces have two serious limitations: (a) The intensity of the scattered light from ultra thin films and the interfaces intermixed to a few atomic layers may be less than the detection limit; (b) A lower penetration depth of the exciting visible light can prevent the investigation of deep buried layer interfaces. However, the first limitation has been overcome to a great extent using an optical interference technique termed as Interference Enhanced Raman Spectroscopy (IERS)[22,23].

IERS is basically an anti-reflection structure consisting of three layers as shown in Figure 1. Using this trilayer, more amount of light can be trapped in the ultra thin layer to be studied (as well as in their interfaces) of thickness less than the penetration depth of the incident light. In this multilayer structure, three different optical functions can be illustrated: (i) The bottom layer is a reflector (normally **Al**) for the exciting laser wavelength (λ), (ii) the second layer above that is a transparent dielectric film (normally SiO_2) which introduces the required phase shift (hence also called as phase layer) and

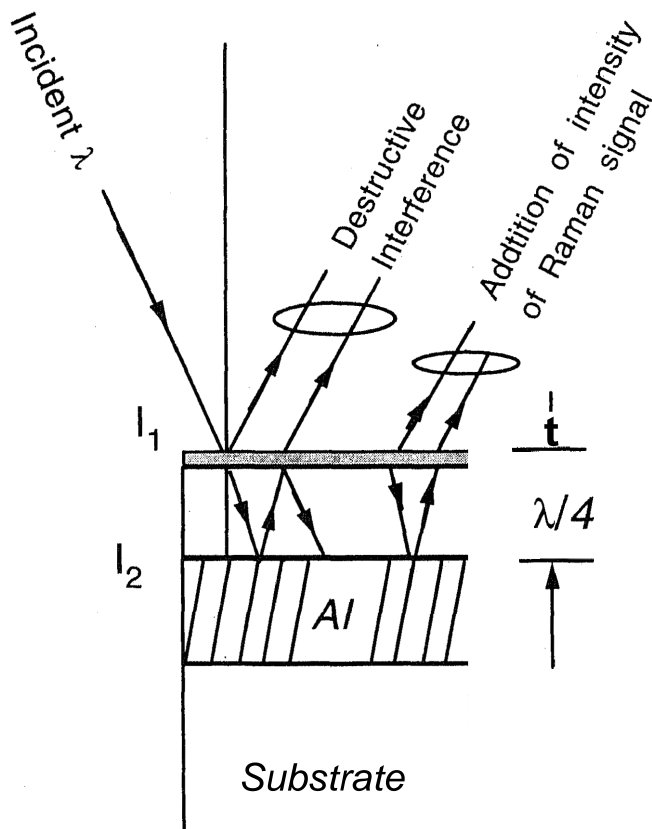

Figure 1. Schematic diagram of trilayer structure.

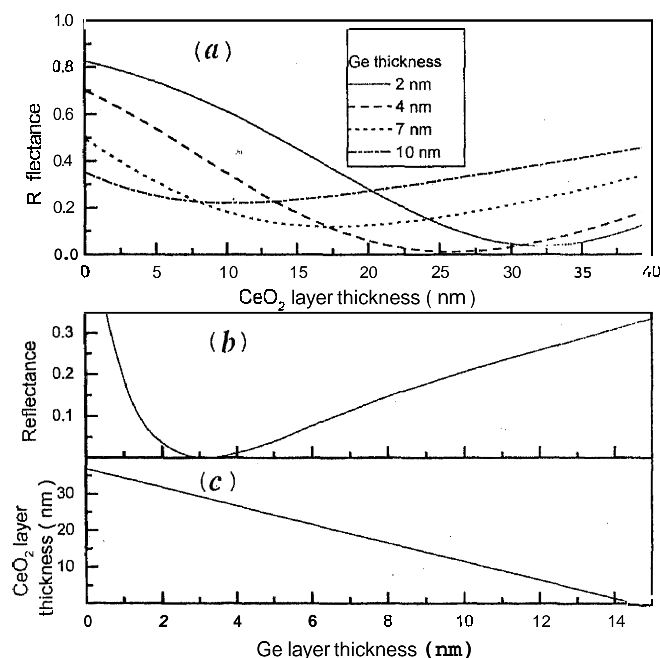

Figure 2. ***a***, Calculated optical reflectance of the trilnyers with various Ge/CeO_2 thickness combinations. ***b***, Calculated values of minimum reflectance as a function of Ge film thickness for optimal thickness of CeO_2. ***c***, Optimal thickness of CeO_2 phase layer as a function of Ge film thickness.

(iii) the ultra thin absorbing layer(s) to be investigated is(are) grown over the dielectric film. In this structure, if the sum of the optical thickness of the dielectric layer and the absorbing layer(s) is equal to $\lambda/4$, then an effective antireflection condition is achieved. Since the base layer is a good reflector and the absorption of the dielectric layer is negligible, most of the incident light is absorbed in the ultra thin layer(s) (as well as in their interfaces), enhancing the Raman signals manyfold. Amongst the semiconductor ultra thin films studied by IERS are amorphous Si (*a*-Si:H) (ref. 24), a-Ge (ref. 25) and the formation of silicides with titanium[26], molybdenum[27] and palladium[28]. *In situ* IERS studies of Bi thin films have revealed that thin layers are disordered while thicker layers are ordered[13]. In all the earlier reports on IERS, *a*-SiO_2 was used as a phase layer. We found that crystalline Ge (c-Ge) can be grown on top of *a*-SiO_2 only at substrate temperatures $T_s > 300°C$ which leads to undesirable inter-diffusion of Al. The growth of c-Ge can be achieved at a relatively low substrate temperature if the dielectric phase Iayer can also serve as a buffer layer. This led us to choose ceria (*c*-CeO_2) instead of *a*-SiO_2 in the trilayer structure. We have earlier shown that crystalline films of CeO_2 (fluorite structure) can be grown at ambient temperatures[29]. In this paper, we report the phonon confinement effects observed for ultra thin Ge films using IERS.

Experimental details

For a given thickness of Ge film, the thickness of CeO_2 is chosen to achieve maximum absorption (or minimum reflectivity) of the incident light using the matrix method for multilayer thin films". The values used in computations are the complex refractive indices of the crystalline bulk Ge (ref. 31) (5-*i*2.5), bulk Al (ref, 30) (0.82-*i*5.45) at the exciting laser wavelength of 514.5 nm. The ceria has negligible absorption at 514.5 nm and its measured refractive index of 2.37 has been used[29]. Figure 2*a* shows the calculated reflectivity at 514.5 nm of the trilayer structure as a function of the CeO_2 film thickness for given thicknesses of Ge. The chosen Ge thicknesses are 2,4, 7 and 10 nm. It can be seen that for Ge layer thickness of 2 nm, the reflectivity of the trilayer at 514.5 nm is minimurn for a CeO_2 film thickness of 33 nm. For various chosen Ge film thickness, the calculated minimum reflectivity of trilayers constructed with optimal CeO_2 film thickness are plotted in panel *b*. Figure 2*c* shows the required optimal thickness of the CeO_2 films. Guided by these results, the trilayer samples of Al/CeO_2/Ge were prepared as follows (A) Al/330 Å CeO_2/20 Å Ge, (B) Al/260 Å CeO_2/ 40 Å Ge (C) Al/165 Å CeO_2/70 Å Ge (D) Al/100 Å CeO_2/100 Å Ge. The films of CeO_2 and Ge were deposited by argon ion beam sputter deposition (IBSD) onto

an aluminum coated glass substrate prepared separately by evaporation. The details of the IBSD are discussed elsewhere[29]. Briefly, the ceria films were sputtered at a total operating pressure of 0.02 Pa from a stoichiometric CeO_2 target including the oxygen partial pressure of 0.01 Pa. The rate of deposition of CeO_2 was 0.5 Å/s. The target used for the preparation of the Ge films was a 2" diameter single crystal of (111) Ge with purity of 99.999%. The films were deposited at an argon pressure of less than 0.003 Pa with the rate of deposition of 0.26 Å/s. Thickness of the films were estimated based on the calibrated rate of deposition using a Talysurf (Rank Taylor Hobson Ltd.) and the X-ray reflectivity study[32]. The substrate temperature, varying from ambient to 300°C, was controlled with an accuracy of 5°C.

Raman measurements were carried out at room temperature in near backscattering configuration using the 514.5 nm line of an Ar^+ ion laser at a low power of -2 mW in order to avoid the local heating of the sample. A Dilor XY spectrometer equipped with a liquid nitrogen cooled CCD detector was used to collect the signal.

Results and discussions

Figure 3 shows the IERS spectra of Ge films of thickness $d = 4$ nm deposited as a function of substrate temperatures T_s. It can be seen that the film deposited at 60°C shows a broad band at 274 cm^{-1} characteristic of amorphous Ge (ref. 33). At $T_s = 150°C$, the deposited film shows a similar broad band at 277 cm^{-1} together with a peak at 299 cm^{-1}, indicating the coexistence of amorphous and crystalline phases of Ge. Pure crystalline films were obtained when $T_s = 225°C$ and higher as indicated by their sharp Raman spectra in Figure 3. The measured full width at half maximum FWHM(Γ) were 10 cm^{-1} and 8.2 cm^{-1} for the films deposited at 225°C and 300°C, respectively, implying that the film deposited at 300°C is better in terms of order and homogeneity. Figure 4 brings out clearly the enhancement of the Raman signal due to the trilayer structure for the films deposited at 300°C, with respect to the Ge films of same thickness coated under identical conditions on CeO_2 but without the Al film. Table 1 lists the enhancement factor with respect to the **bulk** Ge[(100)face] as well as with respect to layer of Ge of the same thickness without IERS structure. For films of thickness of 2 nm, the Raman signal without the Al layer is negligible and hence the enhancement, though not quantified, is rather large.

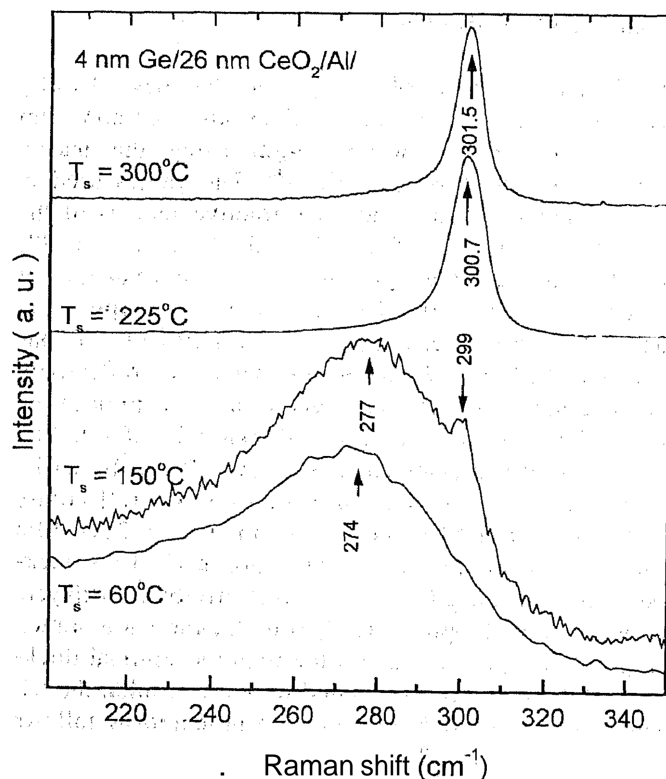

Figure 3. IERS of Ge films of 4 nm thickness as a function of substrate temperatures.

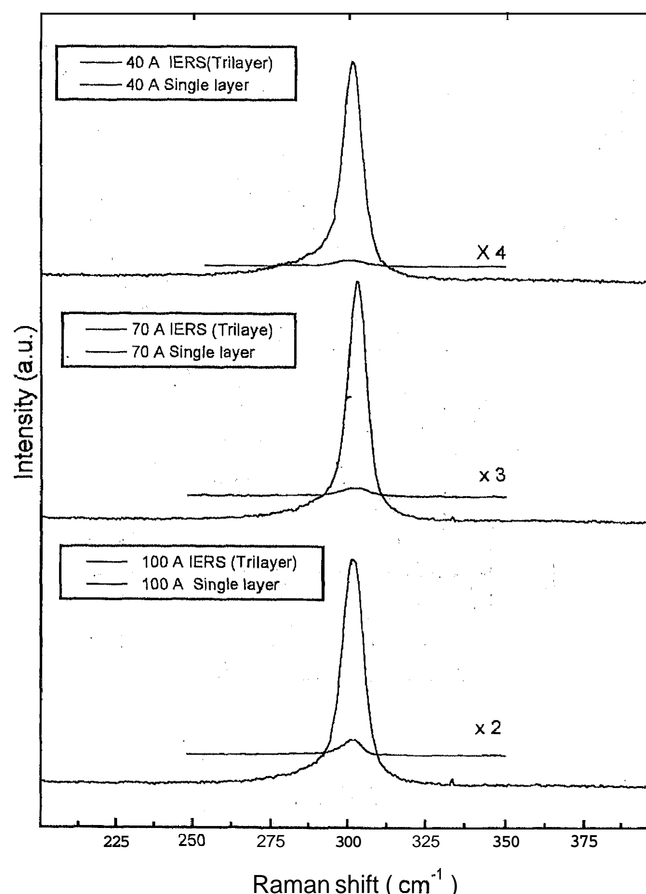

Figure 4. Raman spectra of single layer and trilayer for different Ge film thicknesses.

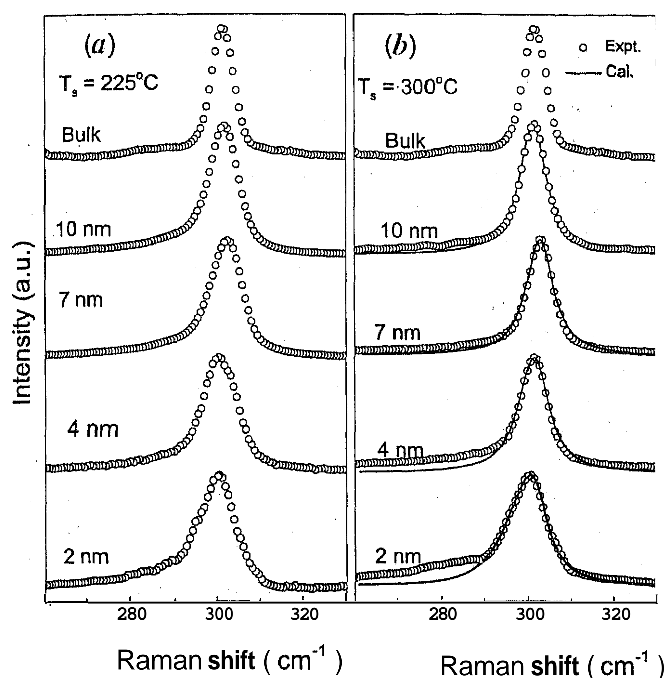

Figure 5. Thickness dependent Raman spectra (IERS) of the Ge films deposited at $T_s = 225°C$ (*n*) and $T_s = 300°C$ (*6*). Also shown line in (*b*) is the calculated $I_c(\omega)$ (eqn. (1)). The calculated curves were shifted in frequency to match the observed peak position.

Table 1. Enhancement factor of IERS signal

Thickness (Å)	Enhancement w.r.t. bulk	Enhancement w.r.t. thin film
20	8.5	–
40	25	65
70	30	39
100	26	31

Figure 5 *a* and *b* show the Raman spectra of c-Ge films of thickness 2, 4, 7 and 10 nm deposited at $T_s = 225°C$ and 300°C. Also shown for comparison is the Raman spectra of bulk Ge(100) single crystal. Figure 6 shows the dependence of peak shift $\delta\omega = \omega(\text{film}) - \omega(\text{Bulk})$ and Γ on the film thickness. The origin of the line broadening and shift as shown in Figures 5 and 6 can be due to the Confinement of the phonon in the growth direction[17,18]. It has been shown that the Raman line shape arising from the phonon confinement is given by[17]

$$I_c(\omega) = D\int_0^{q_{max}} \frac{|C(0,q)|^2 \, dq}{[\omega - \omega(q)]^2 + (\Gamma/2)^2}, \quad (1)$$

where $|C(0, q)|^2$ is the Fourier coefficient of the phonon confinement function, $\omega(q)$ is the phonon dispersion assumed to be the same as for the bulk Ge and Γ_o is the inverse lifetime of the phonon in bulk material.

Taking the confinement to be along the growth direction and the confinement function to be Gaussian[18],

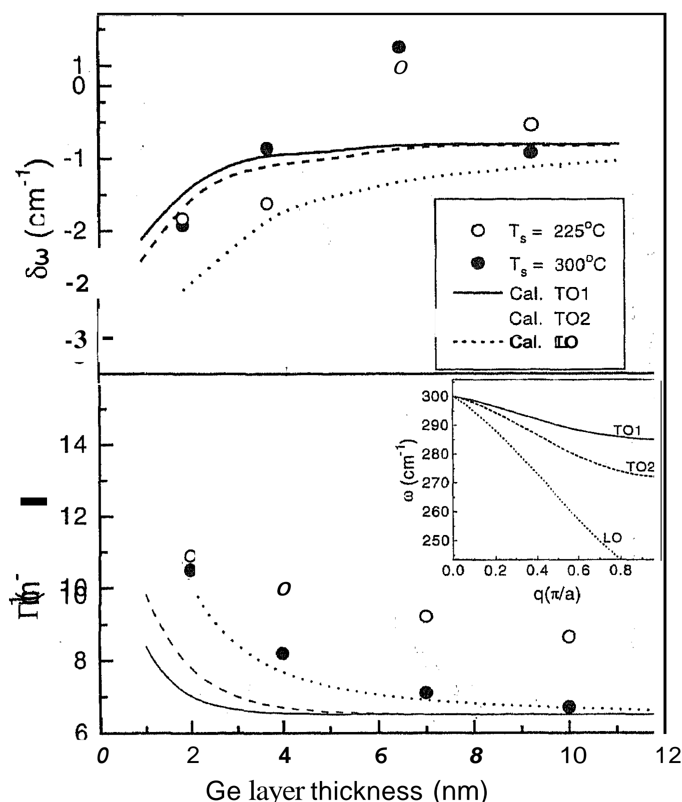

Figure 6. Peak shift $\delta\omega = \omega_{film} - \omega_{bulk}$ and FWHM (Γ) as a function of Ge film thickness. Measured values are shown by open circles (T_s =225°C) and closed circles (T = 300°C). The lines show the calculated values based on $\omega(q)$ for LO, TO1 and TO2 modes of **bulk** Ge. The inset shows the phonon dispersion curves for three phonon branches.

$$|C(0,q)|^2 = \exp\left(\frac{-q^2L^2}{16\pi^2}\right)\left|1 - erf\left(\frac{iqL}{\sqrt{32}\pi}\right)\right|^2, \quad (2)$$

for thin slabs of thickness *L*. It is not clear as to what type of phonon (e.g. longitudinal or transverse) dispersion should be used for ω (*q*). We have, therefore, calculated $I_c(\omega)$ using the $\omega(q)$ for TO1, TO2 and LO in (111) orientation. The measured dispersion of ω as a function of *q* by neutron scattering[34] was well fitted to an empirical equation based on a one-dimensional linear chain model'',

$$\omega^2(q) = A + [A^2 - B[1 - \cos(\pi q^\alpha)]]^{1/2}, \quad (3)$$

where *q* is expressed in units of π/a (**a** = lattice constant = 5.64 Å for Ge), $A = 4.5 \times 10^4$ cm^{-2}, $B = 3.55 \times 10^8 cm^{-4}$ TO1), $5.9 \times 10^8 cm^{-4}$ TO2) and $9.5 \times 10^8 cm^{-4}$ LO) modes and $\alpha = 0.68$ (TO1), 0.71 (TO2) and 0.62 (LO).

The dispersion relations along (11 1) orientation for the three modes are shown as inset in Figure 6. For Γ_o we have used the measured FWHM of 6.5 cm^{-1} for the

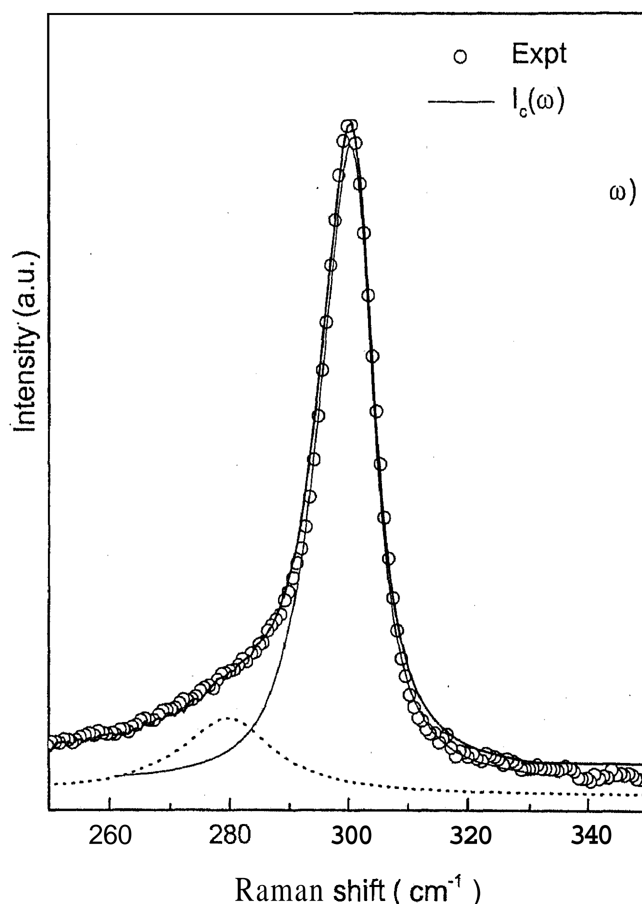

Figure 7. Measured Raman spectra of 2 nm thick Ge films grown at $T_s = 300°C$. $I_c(\omega)$ (shown by dotted line) is due to confined optical phonon and $I_L(\omega)$ (shown by dash) is clue to the surface phonons. The full line shows a sum of $I_c(\omega)$ and $I_L(\omega)$.

bulk Ge which includes broadening due to the instrumental resolution. The values of $\delta\omega$ and Γ were extracted from the calculated $I_c(\omega)$ and are plotted in Figure 6, together with the measured values for the Ge films grown at 225°C and 300°C.

It is seen that the calculated Γ using $\omega(q)$ of the LO mode is very close to the observed values, whereas there is considerable difference between the calculated and observed $\delta\omega$. This difference can be attributed to a contribution arising from the strain in the film (to be discussed later). Now we come to the detailed comparison of the observed line shape ($T_s = 300°C$) with the calculated one using eqs (1–3) (with $\omega(q)$ for the LO mode and $\Gamma_o = 6.5\ cm^{-1}$). Since the peak shift can also arise from the strain, the calculated $I_c(\omega)$ was shifted so as to match the peak positions. Figure 7 shows the comparison of the Raman spectrum of the Ge sample of thickness 2 nm grown at $T_s = 300°C$ with the calculated $I_c(q)$. We observe a significant deviation between the experimental data and $I_c(q)$ on the lower frequency side, similar to the earlier reports[2,36]. The observed line shape can be well fitted (solid line) by a sum of $I_c(\omega)$ (dotted line) and a Lorentian $I_L(\omega)$ (dashed line) centered at -280 cm^{-1}. The origin of the latter will now be discussed. In their study of co-sputtered Ge microcrystals, Fuji *et al.*[36] have argued that the broad Raman band observed at - 280 cm^{-1} is from the disordered surface layers of microcrystals. Sasaki and Horie[33] have carried out resonant Raman study of phonon states in gas evaporated Ge particles. Their deconvoluted spectrum could be decomposed into four Gaussian shaped lines. It was suggested that the line at –280 cm^{-1} can arise from *a-Ge* or nanoparticles of 1 to 2 nm or the Ge with structure different from the diamond lattice. Gaisler *et al.*[37] have also observed an additional band on the low frequency side in the Raman spectra of bulk Ge crystal at 77 K and have assigned this to the vibrations of atomic layers near the surface. In our study, the deviations in the line shape between the observed and the calculated $I_c(\omega)$, seen on the low frequency side, reduced as the Ge film thickness was increased (Figure 5 *b*). Since the deposition conditions were the same, we infer that the additional mode at -280 cm^{-1} could not be attributed to *a-Ge* or structure other than the diamond lattice. We, therefore, attribute this mode to the surface phonon states. The increase in deviation between the obtained data and $I_c(\omega)$ on low frequency side with decreasing Ge thickness arises from the increased surface area to volume ratio.

As far as the variation of $\delta\omega$ with film thickness is concerned (Figure 6), we first compare the bulk and the films deposited at 300°C. As noted before, the observed variation of $\delta\omega$ as a function of thickness does not agree with the calculated line shift based on the phonon confinement. We note that the calculated $\delta\omega$ (using LO dispersion) is higher than the experimental values for all the samples of different thicknesses, indicating that the films are under compressive strain. The origin for such strain is the lattice mismatch between Ge (lattice constant = 5.64 Å) and CeO_2 (lattice constant = 5.41 Å) which can be as large as 4.5%. The films have been deposited at 300°C and the difference in thermal expansion coefficients can also induce thermal strain. This will be of tensile nature and hence will compensate to some extent the above referred compressive strain. Fuji *et al.*[36] studied thermal annealing effects on Ge microcrystals embedded in SiO_2 matrix and observed more blue shift for smaller microcrystals. The magnitude of the blue shift was reduced with the increase of the crystallite size. It was argued that it may be because of compressive strain due to the difference in nearest neighbour distances between Ge–Ge and Si–0.

The frequency shift $\delta\omega$ of a single vibration of frequency ω_o induced by the strain is given by[38],

$$\delta\omega = (p/2\omega_o)\varepsilon_{zz} + (q/2\omega_o)(\varepsilon_{xx} + \varepsilon_{yy}), \quad (4)$$

where the phenomenological parameters for Ge (refs 39, 40) are $p = 1.328 \times 10^5$ cm^{-2}, $q = -1.741 \times 10^5$ cm^{-2}, and ε_{ij} is the strain component and $\omega_0 = 301.6$ cm^{-1}. For a strain = –4.5%, eq. (4) gives the calculated blue shift ($\delta\omega$) as 37.5 cm^{-1}. Cerdeira *et al.*[39] have indeed observed a large frequency shift in MBE grown Ge_xSi_{1-x} superlattices and the frequency shift increased nearly linear with the composition x or the strain. Sutter *et al.*[41] have observed a shift of +14 cm^{-1} in first order LO line of Si_m/Ge_n superlattices. In our case the obtained shift attributed to the strain is much less than 17.5 cm^{-1}, indicating that the films are relatively less strained than 4.5%. This can be due to the incoherent polycrystalline growth of Ge on polycrystalline ceria. The change in $\delta\omega$ as a function of thickness showed that the films were compressively strained up to a thickness of –7 nm beyond which the strain is released. Therefore, the observed variation in $\delta\omega$ should be due to the combined cffcct of both phonon confinement and strain.

In summary, ultra thin crystalline Ge films have been studied using IERS as a function of film thickness to understand confinement-induced changes in Raman spectra-. The conventional phase layer of a-SiO_2 has been replaced by crystalline ceria in order to grow crystalline Ge at relatively low substrate temperatures. It is found that pure crystalline films are grown at substrate temperatures of 225°C and higher. The observed Raman line shape was explained based on the phonon confinement together with an additional Raman mode at 280 cm^{-1} attributed to the surface phonons. The Raman peak position has contributions arising from the phonon confinement and lattice mismatch strain. Using IERS we have also studied *in situ* monitoring of Ge ultra thin layers and the growth of Ge/Si and Si/Ge with and without a surfactant layer[42], showing that IERS is a powerful method in studying vibrational fingerprints of ultra thin semiconducting films.

1. Pearsall, T. P., Bevk, J., Feldman, L. C., Bonar, J. M. and Mannearts, J. P., *Phys. Rev. Lett.*, 1987, **8**, 729.
2. Pearsall, T. P., Vandenberg, J. M., Hull, R. and Bonor, J. M., *Phys. Rev. Lett.*, 1990, *63*, 2104.
3. Zachai, R., Eberl, K., Abstreiter, *G.*, Kasper, E. and Kibbel, H., *Phys. Rev. Lett.*, 1990, **64**, 1055.
4. Canham, L. T., *Appl. Phys. Lett.*, 1990, 57, 1046.
5. Maeda Yoshimito, *Phys. Rev.*, 1995, **51**, 1658.
6. Pearsall, T. P., *Crit. Rev. Solid State Mater. Sci.*, 1989, **15**, *551.*
7. Cardona, M., *et al. Light Scattering in* **Solids,** Springer Verlag, Berlin, 1989, vol. 5.
8. Klein, M. V., *IEEE J. Quant. Elec.*, 1980, **QE22**, 1760.
9. Sood, A. **K.**, Menendeze, J., Cardona, M. and Ploog, K., *Phys. Rev. Lett.*, 1985, **54,** 2115.
10. Sood, A. **K.,** Menendeze, J., Cardona, M. and Ploog, K., *Phys. Rev. Lett.*, 1985, **54,** 2111.
11. Santos, **P.** V., Sood , A. K., Cardona, M. and Ploog, K., *Phys. Rev.*, 1986, 37, 6381.
12. Burger, H., Schaffler, F. and Abstreiter, G., *Phys. Rev. Lett.*, 1984, ***52,*** 141.
13. Mitch, M. G., Chare, S. J., Fortner, J., Yu, **R.** Q. and Lannin, J. S., *Phys. Rev. Lett.*, 1991, **67**,*875.*
14. Wagner, V., Drews, D., Esser, N., Zahn, D. R. T., Geurts, J. and Richter, W., *J. Appl. Plzys.*, 1994, 75, 7330.
15. Drews, D., Langer, M., Richter, W. and Zahn, D. R. T., *Phys. Status Solidi*, 1994, **145,** 491.
16. Zahn, D. R. T., *Phys. Status Solidi*, 1995, **152** , 179.
17. Fauchet, P. M. and Campbell, I. H., *Crit. Rev. Solid State Mater. Sci.*, 1988, 14, S79.
18. Richter, H., Wang, Z. P. and Ley, L., ***Solid** State Commun.*, 1981, **39,** 625.
19. Klein, M. C., Hache, F., Ricard, D. and Flytzanis, G., *Phys. Rev.*, 1990, **42,** 11123; Nomura, S. and Kobayashi, T., *Phys. Rev.*, 1992, **45**, 1305.
20. Roca, E., Trallero-Giner, C. and Cardona, M., *Phys. Rev.*, 1994, **49,** 13704; Chamberlain, M. **P.,** Trallero-Giner, C. and Cardona, M., *Phys. Rev.*, 1995, **51,** 1680.
21. Krauss, T. D., Wise, F. W. and Tanner, D. B., *Phys.* ***Rev.*** *Lett.*, 1996, **76**, 1376.
22. Nemanich, R. J., Tsai, *C.* C. and Connel, G. **A.** N., *Phys. Rev. Lett.*, 1980, **44**, 273.
23. Connell, G. A. N., Nemanich, R. **J.** and Tsai, C. C., *Appl. Phys. Lett.*, 1980, 36, 31.
24. Tsai, *C.* C. and Nemanich, **R.** J., *J. Non. Cryst. Solids*, 1980, 35 and 36, 1203.
25. Fronter, J., Yu, R. Q. and Lannin, J. S., *Plzys. Rev.*, 1990, **42,** 7610,
26. Flucks, R. **J.**, Stafford, B. L. and Vanderplas, H. A., *J. Vac. Sci. Technol.*, 1985, 3, 938.
27. Donald, C. M. and Nemanich, R. J., *J. Mat. Res.*, 1980, 5, 2854.
28. Nemanich, R. J., Tsai, C. C., Thompson, M. J and Sigmon, T. W., *J. Vac. Sci. Techol.*, 1981, **19,** 685.
29. Kanakaraju, S., Mohan, S. and Sood, **A.** K., *Thin Solid Films*, 1997,305, 191.
30. Heavens, **O.** S., *Optical Properties of Thin **Solid** Films*, Butterworths Scientific Publications, London, 1955.
31. Aspens, D. E. and Studna, **A. A.,** *Phys. Rev.*, 1983, **27,** *985.*
32. Bannerjee, S., Sanyal, M. K., Datta, A., Kanakaraju, S. and Mohan, S., *Plzys. Rev.*, 1996, **54,** 377.
33. Sasaki, Y. and Horie, C., *Phys. Rev.*, 1993, **47,** 3811.
34. Nilsson, G. and Nelin, G., ***Phys. Rev.***, 1971, 3, 364.
35. Parayanthal, P. and Pollak, F. H., *Phys. Rev. Lett.*, 1984, ***52,*** 1822.
36. Fuji Minoru, Hayashi Shiniji and Yamamotto Keiichi, *Jpn. J. Appl. Phys.*, 1991, **20,** 687.
37. Gaisler, V. **A.,** Neizvestayi, I. G., Sinyukor, M. P. and Talochlein, A. B., *JETP Lett.*, 1987, **45,** 441.
38. Cerdeira, F., Buchennuuer, C. **J.,** Pollak, F. H. and Cardona, M., *Plzys. Rev.*, 1972, **2,** 580.
39. Cerdeira, F., Pinczuk, **A.,** Bean, J. C., Batlog, B. and Wilson, B. A., *Appl. Phys. Lett,*, 1984, **45,** 1138.
40. Hida, Y., Tamagawa, T., Ueba, H. and Tatsuyama, C., *J. Appl. Plays.*, 1990, **67,**7274.
41. Sutter, P., Schwarz, C., Muller, E., Zelezny, V., Gonacalves-Conto, S. and Von Kanel, H., *Appl. **Phys.** Lett.*, 1994, 65, 2220.
42. Kanakaraju, S., Ph D Thesis, Indian Institute of Science, Bangalore, 1997.

ACKNOWLEDGEMENTS. We thank D. V. S. Muthu for his help in recording the Raman spectrum and DST for financial assistance. We thank *S.* Balaji for his help in preparation of the manuscript.